Evaluation of an Axially and Radially Viewed Inductively Coupled Plasma Using an Échelle Spectrometer With Wavelength Modulation and Second-derivative Detection*

Yoshisuke Nakamura, Katsuyuki Takahashi, Osami Kujirai and Haruno Okochi
National Research Institute for Metals, 2-3-12, Nakameguro, Meguro-ku, Tokyo 153, Japan

Cameron W. McLeod
Department of Chemistry, Sheffield Hallam University, Sheffield, UK S1 1WB

A high-dispersion échelle spectrometer which incorporates wavelength modulation and second-derivative signal detection is used to view analyte emission from an inductively coupled plasma in both the axial (end-on) and radial (side-on) configurations. Movement of the plasma torch assembly between the viewing positions is computer controlled. Performance characteristics such as background intensity, repeatability, background equivalent concentration, limit of detection, dynamic range and interference effects are reported for 24 elements and in general, measurement in the end-on position produces an improvement in sensitivity. Using end-on measurement, the system is applied to the multi-element analysis of a certified reference water.

Keywords: *End-on measurement; inductively coupled plasma atomic emission spectrometry; échelle spectrometer; wavelength modulation; second-derivative detection*

One of the major areas of interest in inductively coupled plasma atomic emission spectrometry (ICP-AES) is optimization of the plasma operating parameters and spectrometer measuring parameters. Almost all development studies and applications have utilized side-on measurement. As the aerosol is introduced into the central part of the toroidal ICP, end-on measurement could be expected to yield increased emission intensity for the elements owing to the extended source path relative to side-on viewing.

Analytical performance of end-on measurement of a horizontal ICP has been investigated by several groups.[1–3] In the end-on measurements by Demers,[1] the optimum observation region was the same for both single and simultaneous quantification and only r.f. power was compromised in the simultaneous quantification. An air cut-off stream was blown upwards towards the tip of the plasma. Kawaguchi *et al.*[2] used a water-cooled low-flow ICP without a cut-off stream. However, de Loos-Vollebregt *et al.*[3] showed that analytical performance of the water-cooled low-flow ICP during end-on measurement without a cut-off stream was similar to that of a conventional high-flow ICP using side-on measurement.

An échelle spectrometer has been used exclusively for side-on measurements.[4–9] Less spectral interferences are expected with the high-dispersion échelle spectrometer. In the present study, the échelle spectrometer incorporating wavelength modulation and second-derivative detection is used to view analyte emission in both end-on and side-on configurations. Optimum operating parameters and basic performance data for end-on measurement are discussed and a critical comparison is made with conventional side-on measurement. A novel aspect of the instrument is the rapid and automated changeover between viewing positions.

Experimental

Échelle Spectrometer

A Kyoto Koken (Uji, Japan) Model UOP-2 MARK II ICP atomic emission spectrometer was used. Details of this échelle spectrometer have been described elsewhere.[7] The échelle grating was a flat type with 79 grooves mm^{-1}. Reciprocal linear dispersion was 0.031, 0.078 and 0.12 nm mm^{-1} at 200, 500 and 800 nm, respectively. Sequential measurement was used. The width and height of both the entrance and exit slits were 100 and 500 μm, respectively. Signal integration time was 5 s. The spectral lines of 24 elements investigated are summarized in Table 1 in order of wavelength. The spectral lines that showed the highest emission intensity and a Gaussian profile were utilized. The spectral lines thus selected for end-on measurement agreed with those for side-on measurement. Real-time background correction was carried out when wavelength modulation and second-derivative detection were used. The wavelength was modulated sinusoidally by a quartz refractor plate, which was positioned behind the entrance slit. The second harmonic of the modulated signal was detected by a built-in lock-in amplifier. The wavelength modulation width for each element was selected according to the wavelength of emission and plasma background interferences. Minimum background intensity at one side of a spectral line was subtracted from the emission intensity for background correction.[7] An auto-tuning system was used for impedance matching.

Torch System

Movement of the ICP torch assembly between end-on and side-on measurements was computer controlled. Schematic diagrams and dimensions for end-on and side-on measurements are shown in Fig. 1. A Fassel-type torch with a bonnet and a cross-flow nebulizer were used. Flow rates of the Ar outer gas, intermediate gas and cut-off stream (end-on measurement) were 15, 1.1 and 10 $dm^3\ min^{-1}$, respectively. Sample uptake rate was 3.0 $cm^3\ min^{-1}$. The shape and position of the drain tubing from a Scott-type spray chamber were modified to allow easy drainage in end-on and side-on measurements. The distance between the torch and entrance slit was 550 mm in side-on measurement, and this was adjusted to between 550 and 610 mm for end-on measurement. With end-on measurement, the central axial region of the ICP was projected onto the entrance slit and fine lateral adjustment was made in order to locate the best ratio of signal-to-standard deviation of background intensity (S/σ) for the analyte. The S/σ was used instead of signal-to-background ratio (S/B) because the background was corrected with real-time background correction and became almost zero and the noise contribution became large.[9] The σ-data acquisition had been programmed into the software of the computer system. A Cu cone was positioned between the ICP and the focal lens in end-on measurement.

* Presented at the International Congress on Analytical Sciences, Makuhari-Messe, Japan, August 25–31, 1991.

Table 1 Operating parameters for end-on and side-on measurements for each element

Element	Spectral line/nm	R.f. power/kW		Position/mm		Carrier gas/dm^3 min^{-1}		Modulation width/ $\pm 10^{-2}$ nm	
		End-on	Side-on	End-on distance	Side-on height	End-on	Side-on	End-on	Side-on
Zn	I 213.856*,†,‡	1.4	1.4	590	6	0.35	0.40	1.70	1.02
Sb	I 217.581*	1.5	1.3	590	11	0.42	0.37	1.36	1.36
Cd	II 226.502*,†	1.5	1.2	590	10	0.35	0.40	1.26	1.26
Co	II 228.616	1.5	1.4	590	10	0.35	0.36	1.26	1.08
As	I 228.812*,†	1.1	1.4	610	8	0.42	0.40	1.44	1.62
Ni	II 231.604†	1.3	1.5	580	11	0.40	0.39	1.66	1.85
B	I 249.773‡	1.4	1.5	600	5	0.45	0.40	1.36	1.95
Mn	II 257.610*,†,‡	1.5	1.3	580	11	0.40	0.35	1.20	1.20
Fe	II 259.940*	1.4	1.5	580	11	0.39	0.40	1.40	1.40
Cr	II 267.716*	1.3	1.5	600	8	0.35	0.40	1.84	1.84
Mg	II 279.553*	1.3	1.2	600	9	0.38	0.40	1.89	1.89
V	II 292.403	1.3	1.4	590	9	0.36	0.35	1.76	1.98
Ga	I 294.364‡	1.3	1.3	600	11	0.35	0.33	1.80	1.80
Be	II 313.042‡	1.5	1.0	590	7	0.38	0.40	1.92	1.68
Ca	II 317.933	1.5	1.4	600	11	0.35	0.40	2.16	1.44
Cu	I 324.754*,†,‡	1.3	1.0	590	10	0.35	0.35	1.96	2.20
Ag	I 328.068‡	1.4	1.3	580	9	0.36	0.40	1.47	1.96
Mo	I 379.825	0.8	0.6	560	20	0.40	0.39	1.96	2.24
Al	I 396.153*,†	1.3	1.1	610	12	0.40	0.40	1.74	2.03
Sr	II 407.771	0.9	1.0	600	17	0.40	0.38	2.40	2.40
U	II 409.014	0.8	0.9	590	17	0.40	0.40	2.10	3.00
Ba	II 455.404*,‡	1.3	1.0	590	10	0.35	0.40	2.34	2.68
Na	I 588.995*	1.0	1.0	580	11	0.36	0.40	2.97	3.40
K	I 766.491	1.4	1.2	610	6	0.40	0.40	4.00	3.50

* Spectral line used by Demers.[1]
† Spectral line used by Kawaguchi *et al.*[2]
‡ Spectral line used by de Loos-Vollebregt *et al.*[3]

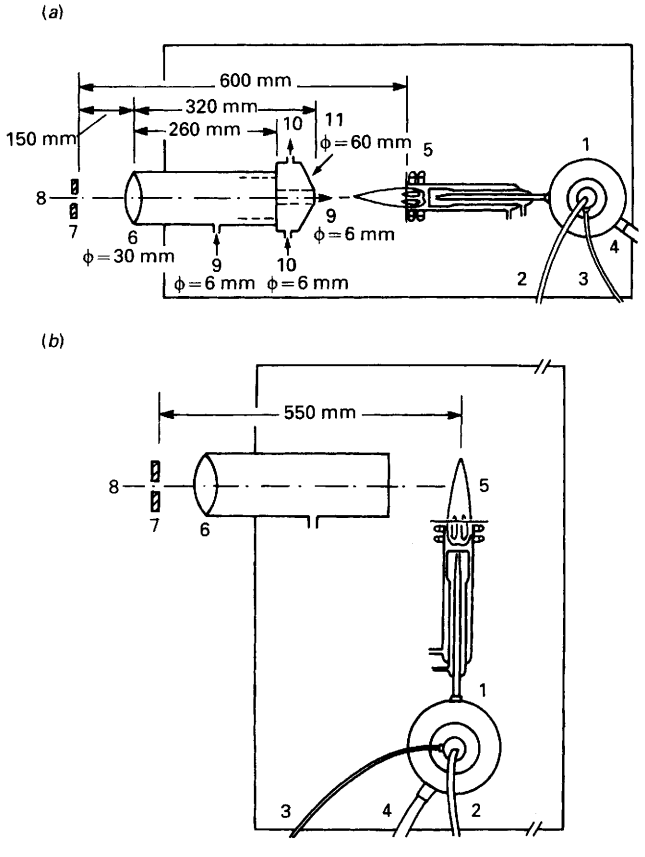

Fig. 1 Schematic diagrams of (*a*) end-on and (*b*) side-on measurements: 1, cross-flow nebulizer; 2, carrier-gas tubing; 3, sample-uptake tubing; 4, drain tubing; 5, ICP torch; 6, focal lens; 7, entrance slit; 8, échelle spectrometer; 9, Ar cut-off stream; 10, cooling water; and 11, Cu cone

Cooling water was circulated through the cone to protect it from over-heating. An Ar cut-off stream was introduced into the cone and passed through the nozzle (6 mm diameter) of the cone against the tip of the horizontal ICP to protect the spectrometer optics from the high temperature and deposits from the sample aerosol.

Reagents and Solutions

Hydrochloric acid, nitric acid, phosphoric acid, sodium chloride and potassium chloride were of analytical-reagent grade. Distilled water was used throughout. Stock solutions (1 g dm^{-3}) of diverse elements were prepared from high-purity metals or compounds (>99.99%, Johnson Matthey, Materials Technology, Royston, Hertfordshire, UK) by dissolving them in minimum amounts of hydrochloric acid and diluting with hydrochloric acid (1+100). Standard solutions were prepared from the stock solutions by serial dilutions. Antimony was dissolved in hydrochloric acid (1+4) and diluted with hydrochloric acid of the same concentration. Silver was dissolved in nitric acid (1+1) and diluted with nitric acid (1+100). Analyte concentrations of 0.10 and 1.0 mg dm^{-3}, respectively, were used for the comparative study of end-on and side-on measurements according to the sensitivity, unless otherwise stated.

A certified reference material (CRM) from the National Research Council of Canada, NRCC CRM SLRS-2 Riverine Water, was analysed.

Measurement

For the comparative study of end-on and side-on measurements, the following operating parameters were used unless otherwise indicated: r.f. power, 1.2 kW; aerosol carrier gas flow rate, 0.40 dm^3 min^{-1}; distance between the torch and the entrance slit (end-on measurement), 600 mm; and wavelength modulation width, 80% of the maximum modulation width.

Dilute standard solutions of each element were used for instrument calibration when analysing the CRM.

Results and Discussion

Establishment of Optimum Operating Parameters

The optimum operating parameters for each element were investigated as follows. Distilled water was nebulized ($n=5$) and the standard deviation (σ) of the background intensity was calculated. Analyte solution was then nebulized ($n=5$) and the average net emission intensity (S) was calculated. The maximum S/σ was used as a criterion for selection of the optimum operating parameters. A univariate study was carried out to select the r.f. power, flow rates of the Ar gas, spectral lines, integration time, slit-width and height, background correction method, modulation width, distance between the torch and the entrance slit (end-on measurement) and the observation height above load coil (side-on measurement). The optimum operating parameters for end-on and side-on measurements thus selected are summarized in Table 1.

Some of the operating parameters will be discussed briefly. It can be seen in Table 1 that the optimum operating parameters differ little from element to element and between end-on and side-on measurements. The distance between the torch and entrance slit in end-on measurement exhibited a maximum S/σ at between 580 and 600 mm for almost all elements. The distance of 600 mm was chosen for the comparative study between end-on and side-on measurements to minimize thermal damage to the Cu cone.

The system allowed for fine adjustment of the plasma torch in the lateral and horizontal directions in order to locate precisely the central axial position. A 10 μg dm^{-3} solution of Sr and distilled water were nebulized ($n=5$ each) and the S/σ was calculated. The S/σ in the centre of the plasma was typically 5-fold better compared with the response at the extremities.

Cut-off Stream

Demers[1] used 50–70 dm^3 min^{-1} of air as the cut-off stream. Argon was used as the cut-off stream in the present study to minimize air entrainment and molecular emission. The effect of the flow rate (4–10 dm^3 min^{-1}) of the Ar cut-off stream was studied on the emission intensities. Although the emission intensities were the same above 6 dm^3 min^{-1}, 10 dm^3 min^{-1} of Ar were used in subsequent studies because 8 dm^3 min^{-1} or more were necessary to blow the tip of the plasma out through the Cu cone nozzle.

Basic Analytical Performance

Background intensity

Background measurements using distilled water were carried out without real-time background correction. The background intensities during end-on measurement were higher than those in side-on measurement by 1.5- to 17-fold except for Be. The background intensity of Be was lower in end-on measurement. Next, the background intensities were measured using real-time background correction. The ratios of background intensities in end-on measurement to those in side-on measurement could be divided into four groups. The ratio of the background intensities was smaller than unity in group I (Be). The background profile showed two small peaks at the shorter and longer wavelength sides of the Be spectral line. The ratios of background intensities in group II (Zn, Sb, Co, Ni, Mn, Fe, Cr, Mg, Ga, Ca, Mo, Al, U and Ba) were around unity. The background profiles showed an irregular plateau which could not be identified as a peak. The ratios of background intensities in group III (V, Ag, Sr and K) were slightly higher than unity and those in group IV (Cd, As, B, Cu and Na) were much higher than unity. The background profiles in group III showed an obscure peak and those in group IV showed a clear peak.

In an attempt to clarify these results, profiles around the spectral lines were investigated. Spectral profiles of the elements that showed relatively high background intensities in end-on measurement are shown in Fig. 2(*a*)–(*f*). The background peaks (broken lines) were reproducible. For example, a strong background peak, which could be partially derived from the Ar 324.755 nm line,[10] was found at the longer wavelength side of the Cu I 324.754 nm line in Fig. 2(*d*). There was a background peak, which could be derived in part from the relatively strong Ar I 588.859 nm line, at the shorter wavelength side of Na I 588.995 nm in Fig. 2(*e*). Fig. 3(*a*)–(*f*) shows the effect of the aerosol carrier gas flow rate in end-on measurement on the background intensities shown in Fig. 2. Two types of experiments were carried out, as shown in Fig. 3, to investigate the effects of the Ar line and OH emission. In one experiment, 3 cm^3 min^{-1} of distilled water (○) were passed through the sample uptake tubing. In another experiment, 3 cm^3 min^{-1} of Ar (●), which is comparable to the sample uptake rate of water, were introduced through the uptake tubing in order not to extinguish the ICP. The background profiles shown in Fig. 3 were the same as those in Fig. 2, although the relationship between the background intensities and the aerosol carrier gas flow rate differed from line to line. It should be mentioned that interference of the OH emission was greater than that of the Ar line at Cu I 324.754 nm in Fig. 3(*d*) and Na I 588.995 nm in Fig. 3(*e*) and *vice versa* at the As I 228.812 nm line in Fig. 3(*b*). Contributions of the Ar line and OH emission differed according to the aerosol carrier gas flow rate at the Cd II 226.502, B I 249.773 and K I 766.491 nm lines in Fig. 3(*a*), (*c*) and (*f*), respectively. Similar but less remarkable behaviour was observed for the background intensities at Cu I 324.754, Na I 588.995 and K I 766.491 nm with side-on measurement.

Stability of the background intensity in end-on measurement is an important factor to evaluate. Distilled water was nebulized and the relative standard deviations (RSDs) of the background intensities ($n=10$) were compared between end-on and side-on measurements using real-time background correction. Although the RSDs ranged from 9.8% for K to 107% for Be in side-on measurement, they ranged from 1.6% for Mg to 36% for Sb in end-on measurement. The RSDs of the background intensities were similarly improved using end-on measurement even if real-time background correction was not used.

Net emission intensity ratio

Ratios of net emission intensities of the 24 elements were compared for end-on and side-on measurements. Standard solutions (1.0 mg dm^{-3} for Sb, As, U and K and 0.10 mg dm^{-3} for the other elements) and distilled water were nebulized and the net emission intensity was obtained by subtracting the background for water. The ratio values of the net emission intensities for end-on to side-on measurement are shown in Table 2. The ratio values for most elements were from 5- to 35-fold. This improvement is mainly due to the increased light flux in end-on measurement. The ratio value for As was low. This small improvement could be due to the fact that the spectral line of As was relatively weak and that the background intensity was relatively high with end-on measurement. Severe spectral interference due to OH emission hindered the side-on measurement of K. However, the increased light flux made the detection of K sensitive in end-on measurement and a high ratio value was obtained.

Repeatability

Repeatability is defined as the RSD of the net emission intensity after background correction ($n=10$). The repeatability for 0.10 mg dm^{-3} solutions of the elements in both end-on and side-on configurations is shown in Table 3. The RSDs for more than half of the elements studied in end-on measurement were less than 3%. However, the RSDs for most elements in side-on measurement were greater than 3%. The RSDs for Sb, As,

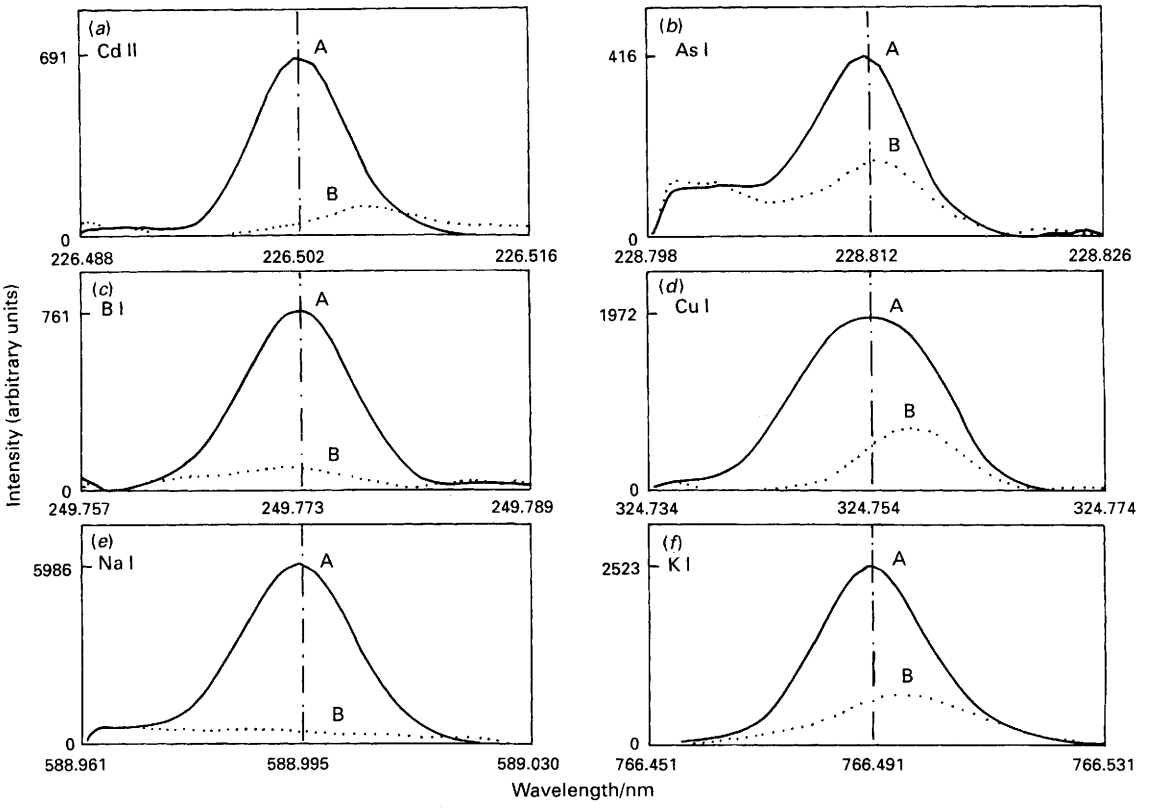

Fig. 2 Spectral profile of background emission in end-on measurement: (*a*) A, 0.10 mg dm^{-3} Cd, B, distilled water; (*b*) A, 1.0 mg dm^{-3} As, B, distilled water; (*c*) A, 0.10 mg dm^{-3} B, distilled water; (*d*) A, 0.050 mg dm^{-3} Cu, B, distilled water; (*e*) A, 0.10 mg dm^{-3} Na, B, distilled water; and (*f*) A, 1.0 mg dm^{-3} K, B, distilled water

U and K in side-on measurement are not shown in Table 3 because the limits of detection (LODs), which will be shown later, were higher than 0.10 mg dm^{-3}.

Background equivalent concentration

The background equivalent concentration (BEC) is defined as the concentration of an element which is equivalent to the background intensity. The BEC values shown in Table 4 were obtained from linear calibration curves without real-time background correction. The BEC values were improved by from 1.4-fold for Mo to 39-fold for Mg by using end-on measurement. The slopes of the calibration curves were steeper in end-on measurement than in side-on measurement. Similar studies were performed using real-time background correction and the slopes of the calibration curves were parallel with and without background correction showing that the decreases in BEC values were equivalent to the background correction.

Limit of detection

The LOD is defined as the concentration equivalent to 3σ of the background intensity using real-time background correction. The LODs obtained are shown in Table 5 for the 24 elements using end-on and side-on measurements. The ratio values of the LODs ranged from 1.4-fold for B to 25-fold for U. Demers[1] obtained 4- to 27-fold improvement in the LODs with end-on measurement. The LODs with end-on measurement were generally lower than those obtained by Demers[1] except for Mn, Fe, Cu, Ba and Na. In the study of Kawaguchi *et al.*,[2] the LODs were 0.7- to 4-fold lower with end-on measurement than with side-on measurement, and improvement of the LODs was greater at shorter wavelengths.[2] However, such a tendency is not seen in the results in Table 5. The LODs obtained in the present study were lower than those reported by de Loos-Vollebregt *et al.*[3] This was due to high RSDs of the noise in the background intensity in the end-on viewed low-flow torch.

The LOD for B was not improved as much with end-on measurement, in spite of the higher emission intensity ratio and better repeatability as shown in Tables 2 and 3. This could be due to the fact that a weak background peak [Fig. 2(*c*)] is located at almost the same wavelength of the B I 249.773 nm line and because of the high background intensity ratio of end-on measurement to side-on measurement. The LOD for K, poor in side-on measurement, was improved in end-on measurement for the same reason as described under net emission intensity ratio.

Comparison of dynamic range

Standard solutions of 0–1000 mg dm^{-3} were used to establish the dynamic range for the 24 elements using real-time background correction. The dynamic range was about four orders of magnitude for Zn, Co, Ni and Al and about five orders of magnitude for Cd, Mn, Mg, V, Cu, Ag and Ba in both end-on and side-on measurements, but lower concentrations could be quantified with end-on measurement. Boron (five orders of magnitude with end-on measurement *versus* seven orders of magnitude with side-on measurement). Fe (four *versus* five), Cr (four *versus* five) and Be (five *versus* six) showed narrower dynamic ranges with end-on measurement than with side-on measurement. Gallium exhibited the same dynamic range (four orders of magnitude) in both measurement modes. Narrower dynamic ranges were obtained in end-on measurements for Ca (five *versus* six) and Na (four *versus* five) and concentrations of about one order of magnitude lower could be quantified with end-on measurement. Antimony (five *versus* four), As (five *versus* four), Mo (five *versus* four), Sr (six *versus* five) and U (five *versus* four) showed wider dynamic ranges with end-on

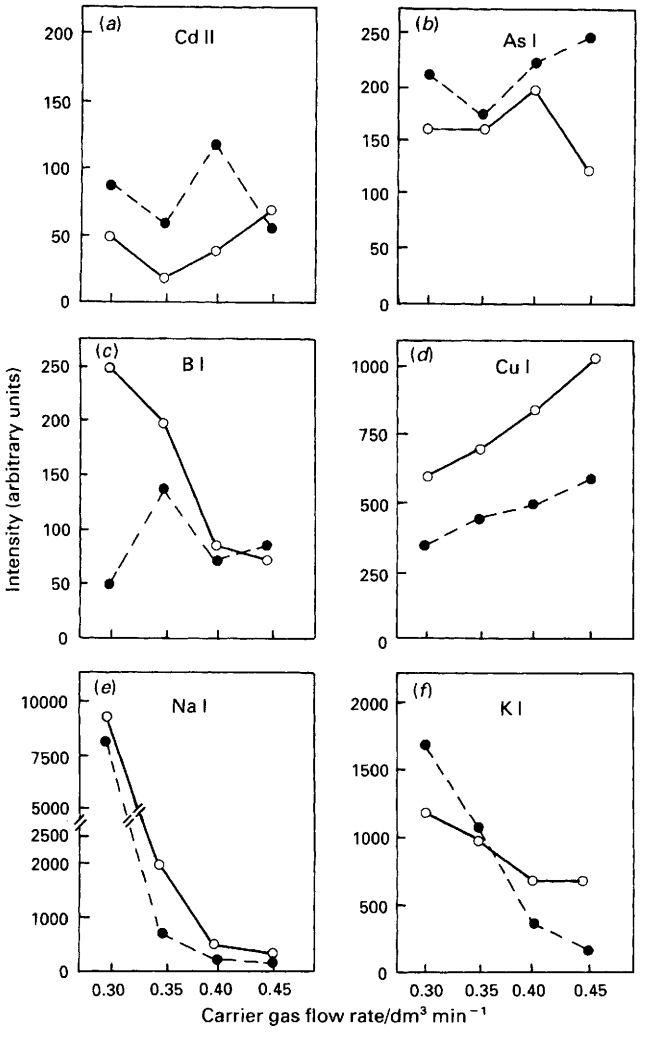

Fig. 3 Effect of aerosol carrier gas flow rate on background intensity in end-on measurement ($n=3$) for: (*a*) Cd II 226.502±0.0144 nm; (*b*) As I 228.812±0.0144 nm; (*c*) B I 249.773±0.0156 nm; (*d*) Cu I 324.754±0.0196 nm; (*e*) Na I 588.995±0.0345 nm; and (*f*) K I 766.491±0.0400 nm. Sample-uptake rate is 3 cm³ min⁻¹ of ○, distilled water and ●, Ar

Table 2 Ratio of net emission intensities in end-on and side-on measurements; $n=3$

Element	Ratio*	Element	Ratio*
Zn	4.9	Ga	5.4
Sb	29	Be	7.2
Cd	17	Ca	20
Co	6.2	Cu	11
As	2.4	Ag	35
Ni	10	Mo	21
B	7.6	Al	29
Mn	26	Sr	14
Fe	9.1	U	31
Cr	33	Ba	11
Mg	16	Na	20
V	26	K	103

* End-on to side-on measurement.

measurement and the concentrations quantified were one order of magnitude lower with end-on measurement. Concentrations of about three orders of magnitude were obtained as the dynamic range for K with end-on measurement.

In general, a lower concentration could be quantified for most elements using end-on measurement than side-on measurement. This could be due to the increased light flu and decreased RSD in end-on measurement. The observatio that a similar dynamic range was obtained for half of th elements studied in end-on and side-on measurements coul be owing to the effect of the Ar cut-off stream. Demers[1] found that the linear dynamic range in end-on measurement wa generally equal or slightly wider than that in side-on measurement. The dynamic range of the calibration curves obtained by Kawaguchi *et al.*[2] was narrower by about one order o magnitude in end-on measurement than in side-on measurement without the cut-off stream. In the study by de Loos-Vollebregt *et al.*,[3] the linear dynamic range in end-on measurement was similar to that in side-on measurement.

Ionization and chemical interferences

Ionization interferences were studied using real-time background correction. Sodium was added at concentrations of up to 10 000 mg dm^{-3}, as an example of an easily ionized interferent, to 1 mg dm^{-3} of a solution of Ca. The effect of Na on the Ca I 422.673 nm line (lower excitation level) was similar to that seen by Demers[1] and larger than that by Kawaguchi *et al.*[2] and the effect on the Ca II 393.367 nm line (higher excitation level) was smaller than that in both of these previous studies[1,2] in end-on measurement.

The effects of Na on two Cr spectral lines (Fig. 4) and on two Cd spectral lines and the effect of K on an Na spectral line (Fig. 5) were studied with end-on and side-on measurements. In Fig. 4, the effect of Na on the relative emission intensity at Cr I 425.435 nm (lower excitation level) was large, especially when the r.f. power was high, and was small on the emission at Cr II 284.325 nm (higher excitation level) in end-on measurement. These interferences were larger than those seen by Demers.[1] The effect of Na was constant on Cr I 425.435 nm up to 10 000 mg dm^{-3} and on Cr II 284.325 nm up to 100 mg dm^{-3} in side-on measurement, even if the observation height was varied. The effect of Na was not observed on Cd I 228.802 nm (lower excitation level) and Cd II 226.502 nm (higher excitation level) up to 1000 mg dm^{-3} of Na against 1 mg dm^{-3} of Cd in both measurement modes. A slightly positive effect of Na was found on Cd I 228.802 nm and Cd II 226.502 nm at 10 000 mg dm^{-3} of Na in end-on measurement although Demers[1] found negative interferences of Na on Cd. In Fig. 5, the large positive effect of K can be seen on Na I 588.995 nm for concentrations of from 100 mg dm^{-3} and greater in end-on measurement and the extent of this effect became larger when the r.f. power increased. The effect of K on Na I 588.995 nm was not observed for up to 1000 mg dm^{-3} in side-on measurement, however, some effects were seen at 10 000 mg dm^{-3} depending on the observation height. These effects of K in side-on measurement were different from the observations made by Demers.[1] The different ionization effects between the present results and those of Demers[1] and Kawaguchi *et al.*[2] are probably attributable to the Ar cut-off stream, real-time background correction and plasma conditions.

Chemical interference of phosphoric acid at up to 3% v/v was investigated on the Ca I 422.673 and Ca II 393.367 nm lines (1 mg dm^{-3} of Ca) in end-on and side-on measurements. The effect of phosphoric acid on the two Ca spectral lines was similar to the results reported by Kawaguchi *et al.*[2]

Analysis of a Water Reference Material

In order to demonstrate the overall reliability of the arrangement used for end-on measurements with this system, the direct analysis of a certified reference water was performed. As shown in Table 6, good accuracy and precision were obtained for four major elements (Mg, Ca, Na and K) and six trace elements (Mn, Fe, Cu, Al, Sr and Ba). Although it had been difficult to quantify trace amounts of Al owing to the recombi-

Table 3 Comparison of repeatability between end-on and side-on measurements for 0.10 mg dm^{-3} solutions; $n=10$

Measurement mode	RSD(%)			
	<1.00	1.00 to 2.99	3.00 to ≈4.99	5.00<
End-on	Mg, Be, Cu, Ag, Sr	Co, B, Mn, Fe, Cr, V, Ca, Mo, Al, Ba	Zn, Cd, Na, K	Sb, As, Ni, Ga, U
Side-on	Be, Sr	Mg, Cu, Ba	Cd, B, Mn, Fe, Cr, V, Ca, Ag	Zn, Co, Ni, Ga, Mo, Al, Na

Table 4 Background equivalent concentrations for end-on and side-on measurements; $n=5$

Element	BEC/mg dm^{-3}		
	End-on	Side-on	Ratio*
Zn	0.0053	0.027	5.1
Sb	0.25	0.42	1.7
Cd	0.024	0.10	4.2
Co	0.044	0.11	2.5
As	0.70	2.14	3.1
Ni	0.057	0.15	2.6
B	0.035	0.42	12
Mn	0.011	0.10	9.1
Fe	0.040	0.12	3.0
Cr	0.014	0.10	7.1
Mg	0.0010	0.039	39
V	0.022	0.13	5.9
Ga	0.16	1.9	12
Be	0.002	0.038	19
Ca	0.053	0.49	9.2
Cu	0.013	0.18	14
Ag	0.027	0.14	5.2
Mo	0.023	0.032	1.4
Al	0.045	0.56	12
Sr	0.0006	0.002	3.3
U	0.23	3.5	15
Ba	0.0044	0.044	10
Na	0.075	2.01	27
K	3.2	12.7	4.0

* Side-on to end-on measurement.

Table 5 Comparison of limits of detection between end-on and side-on measurements; $n=10$, 3σ

Element	LOD/μg dm^{-3}		
	End-on	Side-on	Ratio*
Zn	3.0	16	5.3
Sb	30	540	18
Cd	0.81	6.0	7.4
Co	2.2	23	10
As	29	315	11
Ni	4.6	34	7.4
B	1.6	2.2	1.4
Mn	0.81	4.8	5.9
Fe	4.2	11	2.6
Cr	0.87	5.9	6.8
Mg	0.063	0.30	4.8
V	0.99	3.1	3.1
Ga	16	95	5.9
Be	0.075	0.30	4.0
Ca	0.48	9.9	21
Cu	1.3	4.7	3.6
Ag	0.81	5.7	7.0
Mo	0.72	11	15
Al	2.7	26	9.6
Sr	0.018	0.17	9.4
U	12	300	25
Ba	0.21	1.4	6.7
Na	3.3	34	10
K	35	345	9.9

* Side-on to end-on measurement.

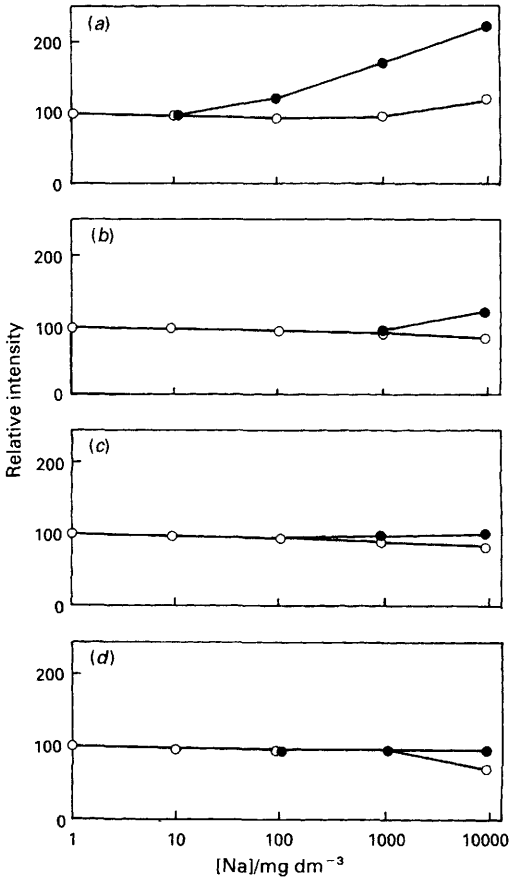

Fig. 4 Effect of Na on Cr emission intensity (1 mg dm^{-3} of Cr); ●, Cr I 425.435 nm, ○, Cr II 284.325 nm: (*a*) and (*b*) end-on measurement for r.f. powers of 1.5 and 1.3 kW, respectively; and (*c*) and (*d*) side-on measurement for r.f. powers of 1.5 W and observation heights of 20 and 9 mm, respectively

nation continuum interference of Ca with side-on measurement, trace amounts of Al in the river water CRM were quantified with end-on measurement. This was due to the high dispersion of the échelle spectrometer, real-time background correction by wavelength modulation and second-derivative detection, and the decreased LOD of Al in end-on measurement.

Conclusions

End-on measurement of the ICP was combined with an échelle spectrometer, which incorporated wavelength modulation and second-derivative detection. This system proved to be more sensitive than side-on measurement, although ionization interferences were rather severe. The system can be switched automatically from end-on to side-on measurement and *vice versa*. However, the optimum operating parameters for end-on and side-on measurements do not normally coincide. The repeatability of net emission intensity was improved in end-on measurement and the LODs were lower in end-on measurement than in side-on measurement. The dynamic range for many elements was almost the same for end-on and side-on

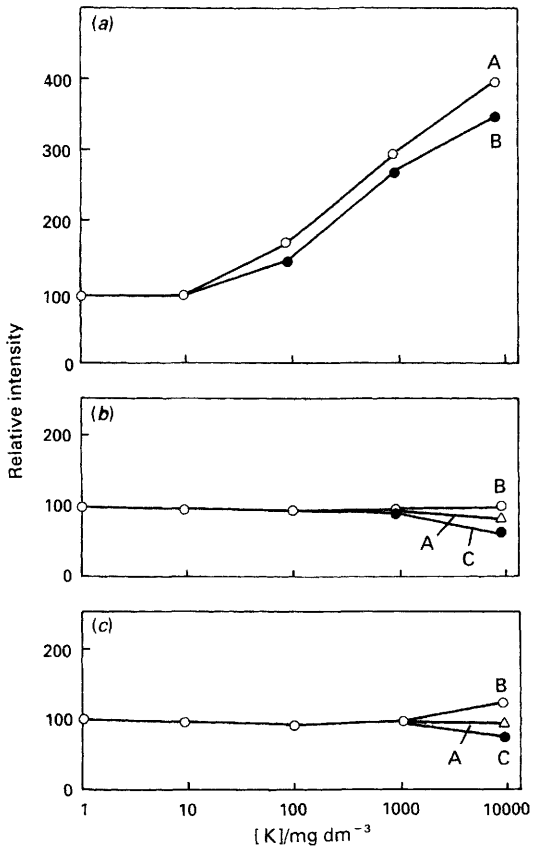

Fig. 5 Effect of K on Na emission intensity (1 mg dm^{-3} of Na) at Na I 588.995 nm. (*a*) End-on measurement at: r.f. powers A, 1.3; and B, 1.0 kW; (*b*) and (*c*) side-on measurement at r.f. powers of 1.0 and 1.3 kW, respectively, at observation heights of A, 4; B, 12; and C, 20 mm

Table 6 Results of river water (NRCC CRM SLRS-2) with end-on measurement; $\bar{x} \pm \sigma$

Element	This work*	Certified value
	Concentration/mg dm^{-3}	
Mg	1.52±0.009	1.51±0.13
Ca	5.67±0.09	5.70±0.13
Na	1.87±0.02	1.86±0.11
K	0.70±0.08	0.69±0.09
	Concentration/μg dm^{-3}	
Zn	<6.0†	3.33±0.15
Sb	<60†	0.26±0.05
Cd	<1.62†	0.028±0.004
Co	<4.4†	0.063±0.012
As	<58†	0.77±0.09
Ni	<9.2†	1.03±0.10
Mn	9.0±0.3	10.1±0.3
Fe	127±2	129±7
Cr	<1.74†	0.45±0.07
V	<1.98†	0.25±0.06
Cu	2.72±0.31	2.76±0.17
Mo	<1.44†	0.16±0.02
Al	83.0±4.0	84.4±3.4
Sr	27.1±0.9	27.3±0.4
U	<24†	0.049±0.002
Ba	14.1±0.2	13.8±0.3

* $n=10$.
† Twice the LOD.

measurements, although quantification at lower concentrations was possible with end-on measurements. Multi-element analysis of a certified reference water was performed successfully. Further studies are needed for other aspects of this system and applications.

The authors thank Kihachiro Murakami of Kyoto Koken, for his cooperation.

References

1 Demers, D. R., *Appl. Spectrosc.*, 1979, **33**, 584.
2 Kawaguchi, H., Tanaka, T., and Mizuike, A., *Bunseki Kagaku*, 1984, **33**, 129.
3 de Loos-Vollebregt, M. T. C., Tiggelman, J. J., and de Galan, L., *Spectrochim. Acta, Part B*, 1988, **43**, 773.
4 Ishii, H., and Satoh, K., *Talanta*, 1982, **29**, 243.
5 Nakamura, Y., and Noto, Y., *Bunseki Kagaku*, 1982, **31**, 413.
6 Ishii, H., and Satoh, K., *Talanta*, 1983, **30**, 111.
7 Nakamura, Y., Takahashi, K., Kujirai, O., and Okochi, H., *J. Anal. At. Spectrom.*, 1990, **5**, 501.
8 Xu, J., Kawaguchi, H., and Mizuike, A., *Appl. Spectrosc.*, 1983, **37**, 123.
9 Berman, S. S., and McLaren, J. W., *Appl. Spectrosc.*, 1978, **32**, 372.
10 Phelps, F. M., III, *MIT Wavelength Tables, Volume 2: Wavelengths by Element*, MIT Press, Cambridge, MA, 1982.

Paper 3/05751H
Received September 23, 1993
Accepted February 24, 1994